

Multi-layer network approach in modeling epidemics in an urban town

Meliksah Turker, Haluk O. Bingol

Abstract—The last two years have been an extraordinary time with the Covid-19 pandemic killing millions, affecting and distressing billions of people worldwide. Authorities took various measures such as turning school and work to remote and prohibiting social relations via curfews. In order to mitigate the negative impact of the epidemics, researchers tried to estimate the future of the pandemic for different scenarios, using forecasting techniques and epidemics simulations on networks. Networks used in these research are either synthetic networks or real networks with limited size and domain specific interactions. Hence, their ability to represent the world is limited. Intending to represent real-life in an urban town in high resolution, we propose a parametric multi-layer undirected weighted network model, where vertices are the individuals of a town that tend to interact locally, and edges represent transmission probability. Each layer corresponds to a different interaction that occurs daily, such as “household”, “work” or “school”, with their own transmission probability. Our simulations indicate that locking down “friendship” layer has the highest impact in slowing down epidemics. Hence, our contributions are twofold, first we propose a parametric network generator model; second, we run SIR simulations on it and show the impact of layers.

Index Terms—Network generator, multi-layer network, complex networks, epidemic, pandemic, Covid-19, SIR.



1 INTRODUCTION

THE study of spread on networks provides insight about how any diffusible—such as disease, idea or gossip—propagates on a network. Understanding the process of diffusion, and the underlying network structure allows taking actions to change the pace of diffusion, such as declaring community lockdown to slow down an epidemic.

Most real-life networks are very complex and large to create an identical twin to study. This complexity leads researchers working on networks to use either synthetic networks whose attributes are similar to real-life networks, or domain specific and limited real-life networks. Despite their similarity to real-world networks, synthetic networks’ ability to represent every real-world interaction is limited. Moreover, domain specific real-world networks are either limited in size or are also too specific to represent every aspect and interaction in life.

Recent Covid-19 epidemic has urged the research on spread on networks [1], [2], [3], [4] and shown the need to model daily life interactions in a high resolution for accurate predictions and right interventions.

In order to support and enhance such studies, we propose a parametric multi-layer network scheme to model the everyday interactions between residents of a hypothetical urban town, modeling individuals and interactions using undirected edge-weighted networks.

In our network, each individual in town is represented by a *vertex*, and any physical interaction between two vertices that may spread a disease is represented by an *edge* with a *weight* corresponding to transmission probability.

Since not all interactions have the same duration or intimacy, different type of interactions pose different transmission probabilities; hence they are represented by different edge weights. For this reason, we adopt multi-layer network approach, where each layer ℓ has its own β_ℓ edge weights.

In each layer of the network, we represent a fundamental relationship in daily life. Following the bottom-up approach, the network is built from the most intimate and enduring relation to lesser ones. In total, the network consists of 7 layers, namely; household, blue-collar workplace, white-collar workplace, school, friendship, service industry, and finally, random encounters.

Moreover, vertices are placed onto locations on the network and interact with their relative neighborhoods. This approach of “locality” allows connecting vertices in a realistic way, rather than randomly, so that they make connections with other vertices by going to work, school, shopping according to where they are, just like the real-world.

The network is defined by two sets of parameters. The first set of parameters define the static, broad structure of the network such as network size, the ratio of workforce, the ratio of vertices that go to school. The second set of parameters define the distributions, values such as household size, number of students in a classroom, number of friends a vertex has, are sampled from. This way, we obtain a diverse and non-homogeneous network, rather than a lattice-like network e.g., where every vertex would live in a house of 4 vertices and have 10 friends. Both sets of parameters are obtained from the real-world whenever possible and assumed plausible values otherwise.

We believe this parametric multi-layer network scheme reflects what happens in an urban town in high resolution and can be used to simulate and inspect different scenarios. The modularity of layers allows answering questions like

• M. Turker and H. O. Bingol are with the Department of Computer Engineering, Bogazici University, Istanbul 34342, Turkey. Email: turkermeliksah@hotmail.com; bingol@boun.edu.tr.

“How helpful is it to turn schools to remote?”, “What would happen if both schools and white-collar jobs turned to remote?”, and “What is the most impactful layer to slow down an epidemic?” by means of inspecting network attributes and running epidemic simulations. We confirm the representative power of our model in two ways. First, our SIR simulation results are aligned with the most recent research and the real-world data [2], [5]. Second, our networks’ attributes are comparable to real-world networks, shown in Sec. 7.8. Moreover, even though the focus of this work is on epidemics due to the recent Covid-19 outbreak, multi-layer network scheme can be used to study other fields on network science such as idea and gossip propagation, social behaviors, and game playing as well.

2 RELATED WORK

Network science has been a widely studied area, especially in the last decades with the increased amount of data. Despite the increasing availability of data, real-world networks are often limited in size, specific to certain domains and static since they are often snapshots taken in a particular moment. Some examples to widely studied real-world networks are Zachary’s karate Club ($N = 34$) [6], Zambian tailor shop ($N = 39$) [7], professional relationships among managers ($N = 21$) [8], relationships among Lazega Law Firm partners ($N = 71$) [9], American football network ($N = 115$) [10], primary school contact network ($N = 236$) [11], where N denotes the number of vertices, or network size. Evidently, real-world networks are frequently two to three digits in size.

Models like Erdős–Rényi [12], Watts–Strogatz [13], Barabási–Albert [14], and random geometric graphs in hyperbolic spaces [15] are able to dynamically and scalably generate networks whose attributes, such as small diameter, short average path length, strong clustering, and community structures are similar to real-world networks [16], [17], [18]. Hence these models are commonly used on network science research.

Several works studied various types of interactions on networks, such as rumor and gossip propagation [19], [20], ideological opinion spread [21], and finally physical, infectious relations that can spread disease [22], [23]. According to common approach in these works, individuals or agents are represented as vertices of the network and interactions or connections between vertices are represented as edges. Therefore, direct propagation of an idea or a disease between two vertices is possible only if they are connected via an edge.

Many researchers [24], [25], [26], [27] working on epidemics on networks considered models like SI, SIS, and SIR where S, I, and R stand for Susceptible, Infected and Recovered/Removed respectively. In these models, an agent can be in one of the mentioned states at a time. Initially, all agents in the population are in susceptible state. Then some selected agents are infected with disease. Susceptible agents that contact infected ones also become infected with transmission probability β . Over time, infected agents either recover or die and get removed from the system, with recovery probability γ . From the perspective of research,

both recovered and removed represent the same state, hence they are used interchangeably and denoted by R.

It is convenient to use weighted networks [25], [26], [28] to represent the transmission probability between two vertices as weighted edge. This way, it becomes possible to model heterogeneous interactions with various transmission probabilities.

Additional to epidemic spread on networks, vaccination on networks is also studied [29], [30], where vaccination is represented by the removal of vaccinated vertices from the network [31], hence rendering vaccinated agents immune, unable to get infected and spread the disease onto other agents.

Multi-layer networks allow representing different type of interactions in different sub-networks or layers. References [32], [33], worked on epidemics on multi-layer networks, where there are multiple graphs or layers that share all vertices but not all edges. Each layer represents a different type of interaction and agents interact through multiple layers. In both of these papers, researchers use variations of SIS and SIR models on top of two-layer synthetic networks, where layers in the prior work are created by Molloy Reed algorithm [34]. Similarly, Buono and her colleagues [35] worked on epidemics on multi-layer complex networks, representing various interactions through different layers, which are also created by Molloy Reed algorithm. In this work, vertices are partially overlapped; therefore, not every vertex exists on every layer of the network. Following these, Wang and his colleagues [27], [36] worked on awareness of epidemics in two-layer networks, generated by Erdős–Rényi and Barabási–Albert models. In these two-layer network schemes, one layer propagates awareness about the disease and the other layer propagates the disease. The impact of awareness on epidemics is studied in single layer networks [37] as well, where both awareness and disease spread over the same network. This work considered Erdős–Rényi [12], Watts–Strogatz [13] and Barabási–Albert [14] models when creating networks. Moreover, a recent work [38] studied evolutionary prisoner’s dilemma on two-layer networks where the researchers used both synthetic and real-world multi-layer networks. Six real-world networks with network size ranging between $N = 21$ to $N = 71$ are studied. In order to obtain larger networks, synthetic networks are created using Erdős–Rényi, Barabási–Albert and Goh–Kahng–Kim [39] models.

Being aware of the difficulty of modeling millions of agents in individual level on a network, a model [40] is proposed to cluster vertices into groups and use these clusters as the high level representation of the network to study epidemics on large scale via approximation. The method is applied to three real-world networks whose sizes vary between $N = 64$ and $N = 236$.

2.1 Covid-19

Covid-19’s emergence and lockdowns interrupted social life widely and brought about more research onto epidemics and networks. Despite their impact on slowing down epidemics, lockdowns and quarantines caused mental and psychological issues on the societies [41]. Naturally, several works studied the effectiveness of precautions and

lockdowns. A relatively early work conducted during the first phase of Covid-19 pandemics [5] inspected the outcome of precautions taken against Covid-19 using statistical methods on evidential real-world data collected worldwide during 2020 and found that cancellation of small gatherings is the most impactful precaution to slow down Covid-19. Following, the impact of collective behavior to end epidemics is studied [1], and it is suggested that blanket cancellation of events that are larger than a critical size can suddenly stop epidemics. Gosak and his colleagues [2] studied whether lockdowns are effective at slowing down epidemics, running SIR model on both synthetic random geometric graphs in hyperbolic spaces networks and real-life network of size $N = 58,000$, obtained by merging phone location data and two online social platforms. The finding of this research is that lockdowns alone have a low impact on slowing down epidemics. Even though it is not a costly precaution like lockdown, the impact of social distancing on epidemics is also studied by Gosak and his colleagues again [3], where the problem in question is formulated as a game theory on networks. In this work, SEIR simulation on synthetic random geometric graphs in hyperbolic spaces network is run and the results suggest that contact and social distancing is not static as authorities and other researchers assume it to be, and endogenous social distancing should be taken into account.

Two papers from 2021 [42], [43] worked on the transmission of Covid-19 and reported that the transmission rate for Covid-19 were 0.13 and 0.17, respectively. Having these quantities is especially important in the perspective of research of epidemics on networks with regards to Covid-19, since it allows leveraging weighted networks with corresponding edge weights to represent transmission probabilities.

The impact of vaccination and prioritization of vaccines in case of short supply is also studied [4], where researchers inspected the efficiency of different vaccination strategies to contain Covid-19, by running SEIRS simulation on synthetic random geometric graphs in hyperbolic spaces network. Their findings suggest that vaccination priority, such as elders first or healthy individuals first, depend on the availability of vaccine and current policy of vaccinating elderly first is beneficial only if vaccine supply is high.

Throughout the literature of network science, it is observed that researchers very frequently work on either limited in size and aspect, domain-specific real-world networks, or synthetic random networks. Our model aims to provide a scalable parametric network generator framework, discussed in Sec. 6, that represents several aspects of physical and social interactions within an urban town to endorse network science research.

The model proposed in this paper leverages multi-layer weighted networks to build its layers. Its multi-layer approach is similar to Buono's [35] in terms of partially overlapping vertices. Moreover, edge weights represent the transmission probability [28], denoted by β . We use a range of β values to simulate various scenarios, including reported Covid-19 transmission rates [42], [43]. Each layer has its own edge weights β_ℓ to represent the various interactions with varying corresponding transmission probabilities. Compared to two-layer approaches in the literature [27], [35],

[36], our model consists of seven layers, each representing a fundamental interaction from daily life. To our knowledge, there is no similar work in the literature in terms of (i) high resolution and representation power offered by the number of layers, (ii) ability to represent diverse interactions in daily life through different layers and transmission probabilities (iii) assignment of vertices to locations on ring lattice and locality of interactions via displacement.

3 METHOD

First, we generate a group of networks to represent various scenarios such as pre-Covid-19 world, remote work, remote school, and complete lockdown. The generator allows us to add or remove layers so that we obtain a family of networks. For example, it is possible to remove the school layer so that students and teachers do not go to school while other interactions remain intact. Then we run SIR disease spreading simulations on each network and compare the disease spread ratios. This gives an indication of how effective it is to lock down the school layer.

3.1 Layered network

As the details are given in Sec. 6, we construct a network that is composed of seven layers. Each layer represents a type of interaction that can be associated with different levels of disease transmission. (L1) *Household layer* corresponds to interactions between households within a house. (L2) *Blue-collar work layer* corresponds to workplace interactions between workers who still had to go to work even during the pandemic lockdown because their jobs require them to be on site. Some examples to this type of work include work performed by workers of sectors such as logistics, manufacturing, and couriers and cashiers of markets and suppliers, as well as doctors and nurses. (L3) Similarly, *white-collar work layer* corresponds to interactions at work, except these interactions being occurring between people who can work remotely via their computers such as office employees, software developers, text translators. There is no difference between blue-collar and white-collar workers normally, but these two-layers allow modeling lockdown and remote working. (L4) *School layer* corresponds to interactions between inhabitants of a school, such as students, teachers, and other employees that work in it.

The first four layers are related to "containers" such as house or school. The remaining three layers are "star" connected. See Sec. 6.2.1 and Sec. 6.2.2 for container and star connections, respectively. (L5) *Friendship layer* corresponds to interactions between friends, such as a meeting between two friends. (L6) *Service industry layer* corresponds to interactions between the employees of service industry, such as couriers and cashiers, and their customers. (L7) *Random encounters layer* corresponds to random interactions between residents of a town that take place while shopping, in a restaurant or cafe, traveling or simply walking by on the street.

Details and parameters of the network generator can be found in sections Sec. 6 and Sec. 7, respectively.

3.2 SIR

Network connectivity depends on the choice of layers. We remove the layers that we want to lock down. Note that the house and blue-collar layers are not sufficient to obtain a connected network. Therefore, disease stays in the connected component, which contains the initial infected vertex. That is, it cannot reach the entire network. Additional layers begin to connect the network.

Having a network that is ready to be inspected, we conduct agent-based SIR simulations, starting from a single infected vertex. Since network connectivity depends on the choice of layers, and the network consists of a wide variety of vertices in terms of spreading potential, this results in a variance in simulation results. We record the *coverage*, which is defined as the ratio of agents that receive the infection. Coverage depends on the initial agent. To account for the worst-case scenario, we consider the agent with the highest *strength* [44], that is, the sum of edge weights of a vertex, from the innermost core [45], [46], [47] of the largest component of the network. In this way, we look for the worst case in the given scenario and stabilize the potential high variance in simulation results that otherwise could be caused by random choice of initial infected vertex. We use *fast_SIR* simulation from Epidemics on Networks EoN package [48], [49], and set recovery rate $\gamma = 1$ for all experiments.

In order not to be specific to a network, which is created by many stochastic processes such as random number generation and sampling from different distributions, we create a new network in each run we take. Therefore, in each run, we create a network with selected parameters, find the best spreader vertex in the largest component and start SIR simulation by infecting this vertex.

4 EXPERIMENTS AND OBSERVATIONS

The median values of 300 realizations in this setting are shown in Fig. 1 where we focus on coverage, the ratio of infected vertices over all vertices. We examine different scenarios starting with *Base*, which consists of layers L1, L2, and L6. We consider this as a baseline scenario since these three layers were the most fundamental layers, persisting even in times of lockdown and curfews for the survival of society.

Then we continue by adding one layer at a time, like (*Base+W*), where we send white-collar agents to work. The combination of multiple letters followed by *Base* indicates that layers corresponding to these letters were active simultaneously in that scenario. For example, (*Base+WS*) means white-collars go to work, schools are open with students and teachers going to classes physically, but curfews still existing with no socialization with friends or neighbors, and no traveling.

As expected, for low values of β , *Base* network by itself is not enough to obtain disease spread. Fig. 1 indicates that we need all layers (*All*) in order to reach a nonzero coverage for $\beta = 0.025$. We need to increase β value to 0.125 in order to get nonzero coverage for *Base* layers only. If we consider adding one single layer to the *Base*, friendship is the first layer to produce nonzero spread at $\beta = 0.05$. At a higher value of $\beta = 0.075$, the *Base* and school pair (*Base+S*)

follows. Then comes *Base* and white-collar (*Base+W*) layers. In fact, the *Base* and friendship combination (*Base+F*) provides the highest coverage compared to all other pairs of single layer on top of *Base*, for $\beta > 0.025$. Considering *Base* and two other layer combinations, *Base*, friendship, and school (*Base+SF*) combination has the highest coverage.

Considering the reported Covid-19 transmission rates $\beta = 0.13$ [42] and $\beta = 0.17$ [43], important observations of Fig. 1 are:

- Disease is able to reach a significant portion ($\approx 40\%$) of the population despite complete lockdown *Base* when $\beta > 0.1$.
- True outbreak with coverage larger than 0.8 occurs in scenarios that include friendship layer when $\beta > 0.1$.
- Friendship layer (*Base+F*) is the single most impactful layer, and even combined white-collar and school layers (*Base+WS*) are not as effective at spreading disease.
- Remote work (*Base+SF*) is not very effective in slowing down disease compared to remote school (*Base+WF*) or restricting socialization with friends (*Base+WS*).
- Majority of the population is infected for all scenarios except *Base*, with reported Covid-19 transmission rates $\beta = 0.13$ and $\beta = 0.17$. The spread reaches almost the entire population when friendship layer is active.
- For high values of $\beta > 0.125$, we observe a saturation above 0.8 coverage for *Base* with any two or more layers.

5 DISCUSSION

Evidential results from real-world data show that the top two most effective non-pharmaceutical interventions (NPI) against Covid-19 are small gathering cancellation and closure of educational institutions [5]. This is consistent with the results of our model, where the most important layer is socialization with friendship layer, followed by the school layer. The high impact of friendship layer arises from two reasons. First, it is an intimate relation with high a transmission rate. Second, and more importantly, it connects clusters of house and work containers that are otherwise disconnected or weakly connected. Both concepts are explained in detail in Sec. 6.

Following that, Gosak's recent work [2] onto the effectiveness of community lockdowns indicates that lockdowns are effective only if communities in the network are disjointed. This is aligned with Fig. 1 where disease is able to spread to about half of the network for reported Covid-19 β values, 0.13 and 0.17, even in the case of *Base*.

5.1 Limitations

Predecessor-successor edges. Our model does not take time into account in terms of predecessor-successor edges. Suppose a susceptible vertex i contacts another susceptible vertex j . Then i contacts the infected vertex k , and gets infected. In this scenario, i is infected after contacting k , therefore, it cannot infect j because it was not infected back

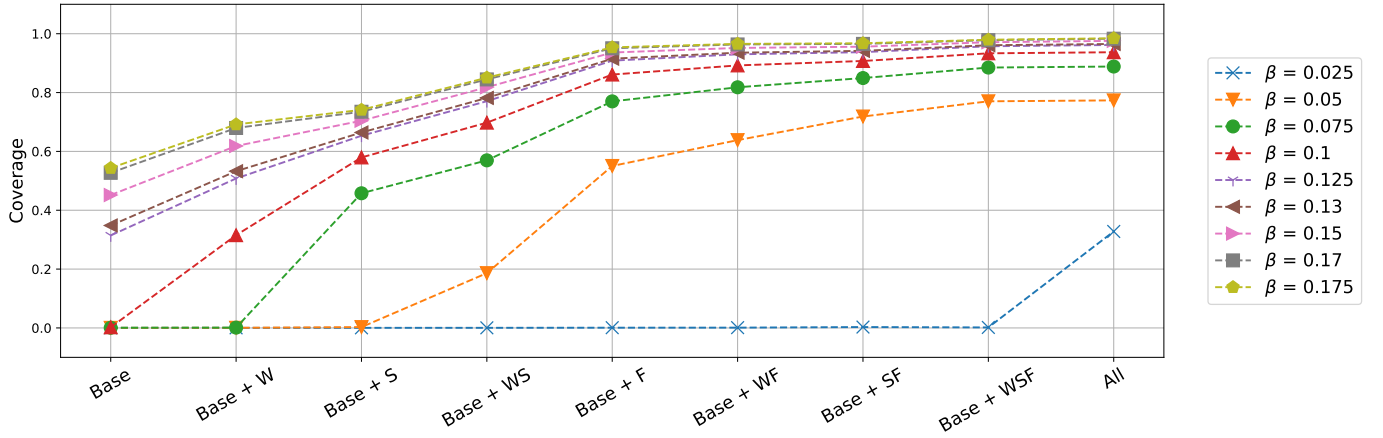


Fig. 1. Median of coverage (300 realizations) as a function of various lockdown scenarios for a range of β values. *X*-axis shows different scenarios. *Base* consists of layers L1, L2, and L6, since these three layers persisted throughout lockdown and curfews. W, S, and F stand for white-collar, school, and friendship layers respectively. Combinations of these, such as WF indicate denoted layers are active simultaneously. “All” indicates the pre-Covid-19 world with no restrictions at all. *Y*-axis shows *coverage*, that is, the ratio of the population infected compared to the whole population. Prominent observations are: (i) for real-life β values of Covid-19, significant portion of the population is infected despite lockdowns and (ii) Friendship is the most impactful layer to spread a disease.

then. Our framework does not model this type of time dimension when creating edges.

Gaussian distribution. We use a set of parameters, some of which define distributions that are used throughout network creation process. If a distribution is known, we use it, as in the case of household size distribution, which is right-skewed Gaussian distribution [50]. If it is not known, we assume it is Gaussian.

Locality. In our model, most of the interactions prefer locality, that is, an interaction between two distant vertices is unlikely compared to an interaction within the neighborhood. Therefore, we assume that all distance measures come from Gaussian distribution with $\mu_d = 0$ and $\sigma_d = 1000$ for all layers. We have no information about how strong locality is for different layers in real-life.

Exponentials of β . We assume different types of interactions have different β transmission probabilities and simplify this by using exponentials of β in different layers. In this way, β decays rapidly from intimate relations to short-duration ones. This is plausible when comparing a contact of 8 hours with one of 30 seconds, but it is still an assumption.

5.2 Future Work

Diffusable spread on networks. Even though the experimental focus in this work has been onto Covid-19 due to the recent pandemic, proposed model can be used to inspect the spread on networks of virtually any diffusable such as disease, gossip, idea. Parametric weighted network structure especially facilitates research on disease spread, e.g., future variants of Covid-19 with corresponding transmission rates.

Vertex assortativity. We assign vertices to houses and create friendship connections randomly, but it may be more realistic to consider assortativity [51] when building these relations as it may be more likely that similar vertices will live together and befriend each other as a result of socioeconomic and demographic factors.

Multiple initial infected agents. Our model starts with all agents in susceptible state except one infected. We try to select the infected one among the agents with the largest spread capacity. The study of initial multiple infected vertices is left for future work.

Multiple towns. This model is designed to inspect single town scenarios in high resolution. To represent a larger scale real-world, multiple towns can be generated with an additional layer where vertices of a town will make connections with vertices in another town to represent travel. Such a model can help understand the transmission of disease between towns and countries [52].

Advanced variants of SIR. In this work, we used the simple SIR model. More sophisticated variants such as SIRS, SEIR and MSIR can be run on our model for more detailed and realistic analysis of disease spreading.

6 NETWORK GENERATOR

6.1 Concepts

We begin by explaining the concepts on which we build our multi-layer network. Note that the terms agent and vertex are used interchangeably.

6.1.1 Interaction types

Close contact between a susceptible and infected creates a potential for disease to spread from infected to susceptible. This potential is implemented by the transmission probability. However, not all real-life contacts are equally intimate, or of equal duration, so they must be assigned transmission probabilities accordingly.

Depending on the potential of disease spreading, we consider 6 types of contacts. They are (i) between households of a house, (ii) between colleagues and co-workers at work, (iii) between students and teachers of a class in school, (iv) between a service provider and taker in service industry, (v) between any two friends, and (vi) between neighbors. Since edges of the network represent these interactions

between vertices, different transmission probabilities are assigned to edges according to the type of the contact.

In terms of network representation, there are two types of interactions.

- i) **Clique.** A *clique* is a group of vertices that are pairwise connected. A *container*, such as house, classroom or workplace, where each agent interacts with every other, are represented as a clique. The number of agents in a container is called *capacity*.

We define containers according to disease transmission probabilities and lockdown possibilities. House has the highest transmission probability among the containers since interactions are more intimate and prolonged. Workplace and classroom should have lower transmission probabilities compared to house. Workplace is divided into two: (i) Essential sectors that cannot be locked down, such as health, logistics, manufacturing, are denoted with *blue-collar* containers. (ii) The sectors that can be locked down during an epidemic, which are further divided into the education sector, denoted by *school* layer, and sectors that can work remotely, which are grouped under the *white-collar* layer.

Therefore we have four layers representing four types of containers, namely, house, blue-collar, white-collar, and school. At each layer, there are a number of containers, such as homes in house layer, classrooms in school layer and businesses in blue and white-collar layers. Agents in a container are connected as a clique. Note that every agent is associated with one home. A retired person is only associated with its home. An agent may also be associated with a second container, such as a classroom if it is a student or teacher, or to a business if it is a professional.

- ii) **Star.** In *star* connection, a vertex i at the center is connected to a group of vertices that are possibly not connected to each other. The number of connections i makes is called *capacity*. Interactions between workers in the service sector, and their customers, any two friends, and any random encounter are represented by star connections. Even though we model friendship as a star connection, it is known that due to triadic closure, friends of a person tend to be friends as well [53]. We leave that to the stochasticity of network generation.

6.2 Locations and Locality

We use 1D ring lattice, where each vertex is of degree $k = 2$, as an auxiliary network. Note that the ring lattice is used to define locations and distances and has no effect on disease transmission.

Distance. Consider *layer 0* in Fig. 2. There are N vertices representing individuals in the town. Vertices are assigned indices $\{0, 1, \dots, N-1\}$. We can define the *distance* between i and j as $|d| \leq N/2$, where

$$j \equiv i + d \pmod{N}.$$

Then the index of the vertex, which is d steps away from vertex i , is $i + d$, where addition is in mod N .

Locality. People tend to work close to their home, attend a nearby school, shop and have friends in the neighborhood.

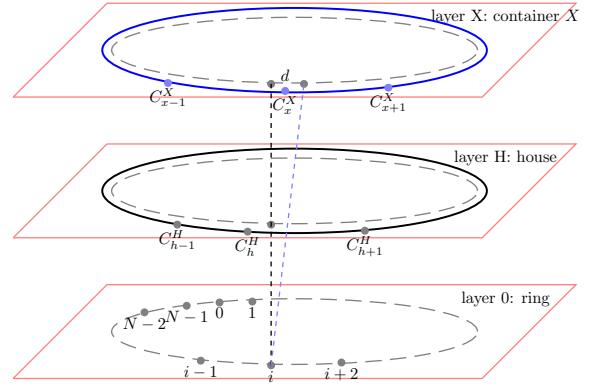


Fig. 2. Multi-layer network scheme with vertices, location and layers of containers. Layer 0 is a 1D ring lattice (N, k) with $k = 2$, that represents the locations of vertices and is used to measure the distance. At the house layer, displacement $d = 0$, therefore agent i is assigned to house h that covers its location. At other container layers X , displacement d can be non-zero, hence it is assigned to the container on $i + d$, e.g., to $x + 1$ instead of x .

This leads us to the *locality*, which can be defined as interactions taking place close to where people live. For example, for small values of displacement d , vertex $i + d$ is in the neighborhood of vertex i . We use this to assign agents to containers and star connections as follows.

6.2.1 Assignment to containers

Consider layer X , such as blue-collar. For agent i on X , assign i to container k if $B_k^X \leq i + d < B_{k+1}^X$, where B_k^X and B_{k+1}^X are the boundaries of the k th container. If there are N_X containers with capacities $\{c_k^X\}_{k=1}^{N_X}$ then the bounds can be calculated by

$$B_0^X = 0, \\ B_k^X = B_{k-1}^X + \frac{c_k^X}{\sum_{\ell=1}^{N_X} c_\ell^X} N \text{ for } k = 1, \dots, N_X$$

as shown in *layer X* in Fig. 2.

Setting the displacement $d = 0$ for house layer puts each agent into its home. For other layers, displacement d is sampled from a Gaussian distribution $\mathcal{N}(\mu_{Xd}, \sigma_{Xd})$, where μ_{Xd} is set to 0 to satisfy locality.

Note that every agent must have a home. Therefore, the total capacity of houses is N . Clearly not every agent must be in a container in other layers. For example, an agent may be in school layer but not in blue-collar layer. Hence, the total capacity of layers blue, white-collar, and school layers is strictly less than the total population. That is, we have $\sum_{k=1}^{N_X} c_k^X \leq N$.

6.2.2 Assignment to star connections

Consider layer X such as friendship layer. For agent i on X , the number of connections k_i is sampled from a Gaussian distribution $\mathcal{N}(\mu_X, \sigma_X)$. For each connection agent i is connected to some $j = i + d$, where displacement d is, as usual, sampled from a Gaussian distribution $\mathcal{N}(\mu_{Xd}, \sigma_{Xd})$. Sampling d is carried out for every connection separately.

See Table 1, Table 2 and Sec. 7 for discussion of parameters N_X , c_k^X , μ_{Xd} , σ_{Xd} , μ_X , and σ_X .

6.2.3 Role assignment

Vertices are assigned to blue, white, and student groups randomly according to their ratio in population, that is Γ_X . For example, in a network where 20 % of the population goes to school, each vertex has 0.20 chance to be labeled as a student. This process is carried out for all containers and vertices.

In case the school layer is active, T teachers are assigned to each class from the nearest work container that contains at least T number of available employees who are not assigned to another class.

7 SETTING PARAMETERS

Network generation requires a number of parameters. Starting by creating a network with $N_H = 10,000$ houses, which corresponds to a network of approximately $N = 26,400$ vertices, see Table 3, we use statistics from the US whenever available and assume plausible values for those that are not. Arbitrary choice of $N_H = 10,000$ is due to the feasibility of computation, hence larger networks can be created with an additional cost of computation and memory. Collected and assumed parameters are shown in Table 1 and Table 2.

7.1 Layer 1. Household

According to ref [50], the average number of households in Turkey is 2.53 with a skewed normal distribution, which is defined by $f(\alpha = 3.96, \xi = 1.22, \omega = 1.75)$ [66] with parameters shape, location, and scale, respectively. According to ref [54], the average household size for the US in 2020 is 2.53. Since we do not know the true distribution of household size for the US but expect it to have very similar characteristics to the distribution for Turkey, which has the same mean, household size is determined by sampling from this distribution.

Since household connections are the most intimate with the highest transmission probability, we assume an infected vertex will surely infect others in its home, therefore we set $\beta_1 = \beta^0 = 1$.

7.2 Layers 2-3. Work

In this work, differentiation between blue and white-collar layers exists solely to be able to modularly model employees who work from home during a lockdown. Hence the only difference between blue and white-collar layers is their ratio in population, Γ_W and Γ_B , and other parameters are the same for both groups.

According to references [58], [59], [60], the number of people interact within a workplace are 9.8, 8 and 5, respectively. We use the mean of these three values, 7.6, as our μ_W and μ_B parameters, and assume σ_W and σ_B to be 3.

Prior to Covid-19, 48 % of the population was in the workforce in the US [55], [56]. This ratio is our baseline when creating jobs and employees. As of January 2021, 56 % of the workforce worked remotely [57]. Using these two data, we obtain the ratios $\Gamma_W = 0.48 \cdot 0.56 = 27\%$ and $\Gamma_B = 0.48 - 0.27 = 21\%$ for white-collars and blue-collars, respectively. Hence, we create workplaces and vertices of white and blue according to these parameters.

Work relations are not as intimate as households, but employees still spend several hours a day together, thus we set $\beta_2 = \beta_3 = \beta^1$.

7.3 Layer 4. School

Even though a school consists of several classrooms where students may also interact and play with students outside the classroom, this is a rather weaker and less likely relation compared to in-class relations, so it is neglected for simplicity and only the interactions in-classroom are modeled in this work.

Ref [61] indicates that $\Gamma_S = 24.7\%$ of the population was enrolled in schools nationwide in 2017. Ref [62] provides the average class size for states in the US. Taking the mean across this sheet for both axes, we obtain $\mu_S = 19.6$. Having no information about this distribution, we assume $\sigma_S = 3$. Although the number of teachers in a classroom depends on the education level and other factors, we simplify this to $T = 3$.

School relations are very similar to work relations in terms of duration and being in containers, so we set $\beta_4 = \beta^1$, as well.

7.4 Layer 5. Friendship

The average number of friends a person has varies according to different sources [63], [64], being 8.6 and 16, respectively. We choose the average of the two and set $\mu_F = 12.3$, and assume $\sigma_F = 5$, which allows both small and large number of friends for different vertices.

Assuming that the friendship relation is at least as intimate as work or school layer, we set $\beta_5 = \beta^1$.

7.5 Layer 6. Service industry

In addition to the first and second layers, one last layer persisted throughout lockdown, virtually everyone still needing essential services such as foods, logistics, health care. Consequently, potentially everyone made connections with workers in these businesses, such as cashiers and couriers. In fact, workers of these essential services were in contact with many people a day. The ratio of service industry workers in population is denoted by Γ_C .

The US Bureau of Labor Statistics provides detailed figures on the US in terms of headcount and demographics for each sector in detail [65]. According to our definition, which is trivially a subset of blue-collar workers, the service industry consists of ‘Wholesale and retail trade’, ‘Taxi and limousine service’, ‘Couriers and messengers’, ‘Real estate and rental and leasing’, ‘Veterinary services’, ‘Services to buildings and dwellings’, ‘Health care and social assistance’, ‘Accommodation and food services’, ‘Other services, except private households’ elements in the “cpsaat2020” table. The total number of people employed in these services divided by the total workforce corresponds to 20 % of the population. However, this is not very accurate for two reasons: First, $\Gamma_B = 21\%$ already, and blue-collar work is not almost entirely made of service industry. Second, not all employees in these sectors are in fact blue-collar workers. Therefore, to make it more realistic and plausible, we multiply this 20 % by a coefficient of $\frac{3}{4}$ and obtain $\Gamma_C = 15\%$, which defines

TABLE 1
Parameters defining layer 1.

Parameter	Value	Description
N_H	10,000	Number of houses
α	3.96	Skewness of household size skewnorm distribution [50], [54]
ξ	1.22	Scale of household size skewnorm distribution [50], [54]
ω	1.75	Location of household size skewnorm distribution [50], [54]
T	3	Number of teachers assigned per class

TABLE 2
Parameters defining layers 2-7, where $\mu_0 = 0$ and $\sigma_0 = 1000$.

Layer	X	Γ_X	μ_X	σ_X	μ_{Xd}	σ_{Xd}	β_X
2: Blue workforce	B	21.0 % [55], [56], [57]	7.6 [58], [59], [60]	3	μ_0	σ_0	β^1
3: White workforce	W	27.0 % [55], [56], [57]	7.6 [58], [59], [60]	3	μ_0	σ_0	β^1
4: Students	S	24.7 % [61]	19.6 [62]	3	μ_0	σ_0	β^1
5: Friendship	F	-	12.3 [63], [64]	5	μ_0	σ_0	β^1
6: Service industry	C	15.0 % [65]	50.0	20	μ_0	σ_0	β^2
7: Random encounters	R	-	50.0	20	μ_0	σ_0	β^3

TABLE 3
Network Attributes.

Network Attribute	Active Layers						
	[L1]	[L1-L2]	[L1-L3]	[L1-L4]	[L1-L5]	[L1-L6]	[L1-L7]
Size of largest component	0 %	47 %	83 %	96 %	100 %	100 %	100 %
Diameter	1.00	38.44	24.78	18.71	9.43	7.45	6.77
Average shortest path length	1.00	16.65	11.32	8.31	4.81	4.14	3.61
Average clustering coefficient	0.66	0.65	0.65	0.70	0.18	0.12	0.05

the number of employees in the service industry who are in active contact with customers.

Since we have no statistical data on how many contacts a service industry worker makes in a given time interval, we assume $\mu_C = 50$ and $\sigma_C = 20$, which has the ability to represent a wide range of jobs.

Compared to other relations, contact between the service provider and customer lasts much shorter. Therefore we set $\beta_6 = \beta^2$, which results in an exponentially lower transmission probability than earlier layers.

7.6 Layer 7. Random Encounters

Interactions people make in daily life do not consist of relations between households, colleagues, students in class, friends known, or cashiers in local stores only. Random encounters with unknown people occur daily during shopping, traveling, or simply walking by another person.

We also have no prior information about the number of random encounters, so we assume $\mu_R = 50$ and $\sigma_R = 20$.

We believe random encounters have even a shorter duration with lower transmission probability compared to six layers defined so far. Thus, we set $\beta_7 = \beta^3$ with an even lower transmission probability.

7.7 Locality

We assume that displacement d for locality comes from a Gaussian distribution $\mathcal{N}(\mu_0, \sigma_0)$. We set $\mu_0 = 0$ so that displacement can be either positive or negative. We assume that $\sigma_0 = 1000$ for all layers 2-7.

7.8 Network Attributes

In this section, network attributes are inspected as layers are added up and are reported in Table 3. The leftmost column indicates the inspected attribute and other columns indicate the layers that are present, such as [L1-L3], which means the first three layers are active and the other four layers are not. Reported numbers are the average values for 300 networks that are generated with the same exact parameters, which are discussed in detail in Sec. 7. In case the network is not connected, the attribute is measured for the largest component of the network.

In the case of [L1], the network consists of disconnected components, hence size of the largest component as % is approximately 0, and the diameter and average shortest path length for the largest component are 1. It is observed that [L1-L3] is sufficient to connect 83 % of the vertices. Further layers improve the connectedness of the network, increasing the size of the largest component and decreasing diameter and average shortest path length.

The network exhibits strong clustering structure for four phases of layers, starting at [L1] and ending at [L1-L4]. The addition of L5 causes a significant drop in both. This behavior is expected since L5 is the first layer that is not container type, and it connects a vertex to several vertices that are part of several containers. This is discussed in Sec. i.

We believe that it is more plausible to take [L1-L5] into account when comparing the proposed model's network attributes to real-life network attributes rather than [L1-L7] or [L1-L6] since L6 and L7 represent exponentially weaker relations as explained in Sec. 7.5, that are ignored in real-life networks. Herewith, inspecting the properties of [L1-L5], it is observed that our model successfully generates networks

that exhibit similar properties to real-life networks, namely small diameter, and average shortest path length and high clustering coefficient [16], [17], [18].

8 CONCLUSION

Witnessing the absence of a high resolution network generator in literature, we offer a parametric multi-layer undirected weighted network scheme to model a hypothetical urban town where individuals and their interactions are represented as vertices and weighted edges, respectively. Multi-layer networks are utilized to represent various interactions with different transmission rates, each layer corresponding to a different fundamental relation in everyday life. The layered architecture makes it possible to lock down different combinations of layers to model scenarios like remote work, remote school, and curfews. First, we run SIR simulations on generated networks for different lockdown scenarios and show that the friendship layer is the most impactful layer to slow down epidemics. Second, we inspect and compare our model's generated networks' attributes to real-life networks. It is observed that our model's attributes and simulation results are aligned with real-life data and the most recent research. This indicates the strength and realism of our network generator model and stimulates network science research.

NETWORK GENERATOR CODE

Source code of the proposed network generator can be accessed at <https://github.com/meliksahurker/NetGen>.

ACKNOWLEDGMENT

We would like to thank Emre Aladag and Samet Atdag for constructive comments. This work is partially supported by the Turkish Directorate of Strategy and Budget under the TAM Project number 2007K12-873.

REFERENCES

- [1] G. St-Onge, V. Thibeault, A. Allard, L. J. Dubé, and L. Hébert-Dufresne, "Social confinement and mesoscopic localization of epidemics on networks," *Physical Review Letters*, vol. 126, no. 9, p. 098301, 2021.
- [2] M. Gosak, M. Duh, R. Markovič, and M. Perc, "Community lockdowns in social networks hardly mitigate epidemic spreading," *New Journal of Physics*, vol. 23, no. 4, p. 043039, 2021.
- [3] M. Gosak, M. U. Kraemer, H. H. Nax, M. Perc, and B. S. Pradelski, "Endogenous social distancing and its underappreciated impact on the epidemic curve," *Scientific Reports*, vol. 11, no. 1, pp. 1–10, 2021.
- [4] R. Markovič, M. Šterk, M. Marhl, M. Perc, and M. Gosak, "Socio-demographic and health factors drive the epidemic progression and should guide vaccination strategies for best covid-19 containment," *Results in Physics*, vol. 26, p. 104433, 2021.
- [5] N. Haug, L. Geyrhofer, A. Londei, E. Dervic, A. Desvars-Larrive, V. Loreto, B. Piniór, S. Thurner, and P. Klimek, "Ranking the effectiveness of worldwide covid-19 government interventions," *Nature Human Behaviour*, vol. 4, no. 12, pp. 1303–1312, 2020.
- [6] W. W. Zachary, "An information flow model for conflict and fission in small groups," *Journal of Anthropological Research*, vol. 33, no. 4, pp. 452–473, 1977.
- [7] B. Kapferer, *Strategy and transaction in an African factory: African workers and Indian management in a Zambian town*. Manchester University Press, 1972.
- [8] D. Krackhardt, "Cognitive social structures," *Social Networks*, vol. 9, no. 2, pp. 109–134, 1987.
- [9] E. Lazega et al., *The collegial phenomenon: The social mechanisms of cooperation among peers in a corporate law partnership*. Oxford University Press on Demand, 2001.
- [10] M. Girvan and M. E. Newman, "Community structure in social and biological networks," *Proceedings of the National Academy of Sciences*, vol. 99, no. 12, pp. 7821–7826, 2002.
- [11] J. Stehlé, N. Voirin, A. Barrat, C. Cattuto, L. Isella, J.-F. Pinton, M. Quaggiotto, W. Van den Broeck, C. Régis, B. Lina et al., "High-resolution measurements of face-to-face contact patterns in a primary school," *PloS One*, vol. 6, no. 8, p. e23176, 2011.
- [12] P. Erdős and A. Rényi, "On random graphs i," *Publicationes Mathematicae Debrecen*, vol. 6, pp. 290–297, 1959.
- [13] D. J. Watts and S. H. Strogatz, "Collective dynamics of 'small-world' networks," *Nature*, vol. 393, no. 6684, pp. 440–442, 1998.
- [14] A.-L. Barabási and R. Albert, "Emergence of scaling in random networks," *Science*, vol. 286, no. 5439, pp. 509–512, 1999.
- [15] M. Boguná, F. Papadopoulos, and D. Krioukov, "Sustaining the internet with hyperbolic mapping," *Nature Communications*, vol. 1, no. 1, pp. 1–8, 2010.
- [16] M. E. Newman, A.-L. E. Barabási, and D. J. Watts, *The structure and dynamics of networks*. Princeton University Press, 2006.
- [17] D. Krioukov, F. Papadopoulos, M. Kitsak, A. Vahdat, and M. Boguná, "Hyperbolic geometry of complex networks," *Physical Review E*, vol. 82, no. 3, p. 036106, 2010.
- [18] K. Zuev, M. Boguná, G. Bianconi, and D. Krioukov, "Emergence of soft communities from geometric preferential attachment," *Scientific Reports*, vol. 5, no. 1, pp. 1–9, 2015.
- [19] D. H. Zanette, "Dynamics of rumor propagation on small-world networks," *Physical Review E*, vol. 65, no. 4, p. 041908, 2002.
- [20] P. G. Lind, L. R. Da Silva, J. S. Andrade Jr, and H. J. Herrmann, "Spreading gossip in social networks," *Physical Review E*, vol. 76, no. 3, p. 036117, 2007.
- [21] A. Volkening, D. F. Linder, M. A. Porter, and G. A. Rempala, "Forecasting elections using compartmental models of infection," *SIAM Review*, vol. 62, no. 4, pp. 837–865, 2020.
- [22] R. M. May and A. L. Lloyd, "Infection dynamics on scale-free networks," *Physical Review E*, vol. 64, no. 6, p. 066112, 2001.
- [23] M. E. Newman, "Spread of epidemic disease on networks," *Physical Review E*, vol. 66, no. 1, p. 016128, 2002.
- [24] Y. Moreno, R. Pastor-Satorras, and A. Vespignani, "Epidemic outbreaks in complex heterogeneous networks," *The European Physical Journal B-Condensed Matter and Complex Systems*, vol. 26, no. 4, pp. 521–529, 2002.
- [25] M. Youssef and C. Scoglio, "An individual-based approach to sir epidemics in contact networks," *Journal of Theoretical Biology*, vol. 283, no. 1, pp. 136–144, 2011.
- [26] C. Kamp, M. Moslonka-Lefebvre, and S. Alizon, "Epidemic spread on weighted networks," *PLoS Computational Biology*, vol. 9, no. 12, p. e1003352, 2013.
- [27] Z. Wang, Q. Guo, S. Sun, and C. Xia, "The impact of awareness diffusion on sir-like epidemics in multiplex networks," *Applied Mathematics and Computation*, vol. 349, pp. 134–147, 2019.
- [28] Y. Gang, Z. Tao, W. Jie, F. Zhong-Qian, and W. Bing-Hong, "Epidemic spread in weighted scale-free networks," *Chinese Physics Letters*, vol. 22, no. 2, p. 510, 2005.
- [29] N. Madar, T. Kalisky, R. Cohen, D. Ben-avraham, and S. Havlin, "Immunitization and epidemic dynamics in complex networks," *The European Physical Journal B*, vol. 38, no. 2, pp. 269–276, 2004.
- [30] Z. Wang, C. T. Bauch, S. Bhattacharyya, A. d'Onofrio, P. Manfredi, M. Perc, N. Perra, M. Salathé, and D. Zhao, "Statistical physics of vaccination," *Physics Reports*, vol. 664, pp. 1–113, 2016.
- [31] R. Albert, H. Jeong, and A.-L. Barabási, "Error and attack tolerance of complex networks," *Nature*, vol. 406, no. 6794, pp. 378–382, 2000.
- [32] V. Marceau, P.-A. Noël, L. Hébert-Dufresne, A. Allard, and L. J. Dubé, "Modeling the dynamical interaction between epidemics on overlay networks," *Physical Review E*, vol. 84, no. 2, p. 026105, 2011.
- [33] F. D. Sahneh, C. Scoglio, and P. Van Mieghem, "Generalized epidemic mean-field model for spreading processes over multilayer complex networks," *IEEE/ACM Transactions on Networking*, vol. 21, no. 5, pp. 1609–1620, 2013.
- [34] M. Molloy and B. Reed, "A critical point for random graphs with a given degree sequence," *Random Structures & Algorithms*, vol. 6, no. 2-3, pp. 161–180, 1995.
- [35] C. Buono, L. G. Alvarez-Zuzek, P. A. Macri, and L. A. Braunstein, "Epidemics in partially overlapped multiplex networks," *PloS One*, vol. 9, no. 3, p. e92200, 2014.

- [36] Z. Wang and C. Xia, "Co-evolution spreading of multiple information and epidemics on two-layered networks under the influence of mass media," *Nonlinear Dynamics*, vol. 102, no. 4, pp. 3039–3052, 2020.
- [37] A. Azizi, C. Montalvo, B. Espinoza, Y. Kang, and C. Castillo-Chavez, "Epidemics on networks: Reducing disease transmission using health emergency declarations and peer communication," *Infectious Disease Modelling*, vol. 5, pp. 12–22, 2020.
- [38] Q. Su, A. McAvoy, Y. Mori, and J. B. Plotkin, "Evolution of prosocial behaviours in multilayer populations," *Nature Human Behaviour*, pp. 1–11, 2022.
- [39] K.-I. Goh, B. Kahng, and D. Kim, "Universal behavior of load distribution in scale-free networks," *Physical Review Letters*, vol. 87, no. 27, p. 278701, 2001.
- [40] B. Prasse, K. Devriendt, and P. Van Mieghem, "Clustering for epidemics on networks: A geometric approach," *Chaos: An Interdisciplinary Journal of Nonlinear Science*, vol. 31, no. 6, p. 063115, 2021.
- [41] A. Sameer, M. Khan, S. Nissar, and M. Bandy, "Assessment of mental health and various coping strategies among general population living under imposed covid-lockdown across world: a cross-sectional study," *Ethics, Medicine and Public Health*, vol. 15, p. 100571, 2020.
- [42] L. Zhang, J. Zhu, X. Wang, J. Yang, X. F. Liu, and X. K. Xu, "Characterizing covid-19 transmission: incubation period, reproduction rate, and multiple-generation spreading," *Frontiers in Physics*, vol. 8, 2021.
- [43] S. Feng, Z. Feng, C. Ling, C. Chang, and Z. Feng, "Prediction of the covid-19 epidemic trends based on seir and ai models," *PloS One*, vol. 16, no. 1, p. e0245101, 2021.
- [44] A. Barrat, M. Barthelemy, R. Pastor-Satorras, and A. Vespignani, "The architecture of complex weighted networks," *Proceedings of the National Academy of Sciences*, vol. 101, no. 11, pp. 3747–3752, 2004.
- [45] S. N. Dorogovtsev, A. V. Goltsev, and J. F. F. Mendes, "*k*-core organization of complex networks," *Physical Review Letters*, vol. 96, p. 040601, 2006.
- [46] M. Kitsak, L. K. Gallos, S. Havlin, F. Liljeros, L. Muchnik, H. E. Stanley, and H. A. Makse, "Identification of influential spreaders in complex networks," *Nature Physics*, vol. 6, no. 11, p. 888, 2010.
- [47] S. Atdag and H. O. Bingol, "Computational models for commercial advertisements in social networks," *Physica A: Statistical Mechanics and its Applications*, vol. 572, p. 125916, 2021.
- [48] J. C. Miller and T. Ting, "Eon (epidemics on networks): A fast, flexible python package for simulation, analytic approximation, and analysis of epidemics on networks," *The Journal of Open Source Software*, 2019.
- [49] —, "Eon (epidemics on networks): a fast, flexible python package for simulation, analytic approximation, and analysis of epidemics on networks," *arXiv preprint arXiv:2001.02436*, 2020.
- [50] I. L. Organization, "Household labor force survey 2017 turkey," 2019, online; accessed 29-May-2021. [Online]. Available: <https://www.ilo.org/surveyLib/index.php/catalog/2659>
- [51] M. E. Newman, "Assortative mixing in networks," *Physical Review Letters*, vol. 89, no. 20, p. 208701, 2002.
- [52] J. T. Davis, M. Chinazzi, N. Perra, K. Mu, A. Pastore y Piontti, M. Ajelli, N. E. Dean, C. Gioannini, M. Litvinova, S. Merler *et al.*, "Cryptic transmission of sars-cov-2 and the first covid-19 wave," *Nature*, vol. 600, no. 7887, pp. 127–132, 2021.
- [53] D. Easley and J. Kleinberg, *Networks, Crowds, and Markets*. Cambridge University Press, 2010.
- [54] Statista, "Average number of people per household in the united states from 1960 to 2020," 2021, online; accessed 29-May-2021. [Online]. Available: <https://www.statista.com/statistics/183648/average-size-of-households-in-the-us/>
- [55] —, "Employment in the united states from 2012 to 2022," 2021, online; accessed 29-May-2021. [Online]. Available: <https://www.statista.com/statistics/269959/employment-in-the-united-states/>
- [56] U. S. Population, "United states population," 2021, online; accessed 29-May-2021. [Online]. Available: <https://www.worldometers.info/world-population/us-population/>
- [57] U. News, "Poll: Americans like working at home," 2021, online; accessed 29-May-2021. [Online]. Available: <https://www.usnews.com/news/national-news/articles/2021-02-12/majority-of-americans-work-remotely-a-year-into-coronavirus-pandemic-poll-finds>
- [58] Gallup, "Americans' social contacts during the covid-19 pandemic," 2020, online; accessed 29-May-2021. [Online]. Available: <https://news.gallup.com/opinion/gallup/308444/americans-social-contacts-during-covid-pandemic.aspx>
- [59] S. Y. Del Valle, J. M. Hyman, H. W. Hethcote, and S. G. Eubank, "Mixing patterns between age groups in social networks," *Social Networks*, vol. 29, no. 4, pp. 539–554, 2007.
- [60] T. Ladders, "Survey: This is the average amount of friends people have in the office," 2018, online; accessed 29-May-2021. [Online]. Available: <https://www.theladders.com/career-advice/survey-this-is-the-average-amount-of-friends-people-have-in-the-office>
- [61] U. S. C. Bureau, "More than 76 million students enrolled in u.s. schools, census bureau reports," 2018, online; accessed 29-May-2021. [Online]. Available: <https://www.census.gov/newsroom/press-releases/2018/school-enrollment.html>
- [62] N. C. for Education Statistics, "National teacher and principal survey," 2018, online; accessed 29-May-2021. [Online]. Available: https://nces.ed.gov/surveys/ntps/tables/ntps1718_ftable06_t1s.asp
- [63] Independent, "Average american hasn't made a new friend in five years, study finds," 2019, online; accessed 29-May-2021. [Online]. Available: <https://www.independent.co.uk/life-style/friends-adults-american-how-friendship-difficulty-a8906861.html>
- [64] Gallup, "Americans satisfied with number of friends, closeness of friendships," 2004, online; accessed 29-May-2021. [Online]. Available: <https://news.gallup.com/poll/10891/americans-satisfied-number-friends-closeness-friendships.aspx>
- [65] U. B. of Labor Statistics, "Labor force statistics from the current population survey," 2020, online; accessed 29-May-2021. [Online]. Available: <https://www.bls.gov/cps/cpsaat18.htm>
- [66] A. Azzalini and A. Capitanio, "Statistical applications of the multivariate skew normal distribution," *Journal of the Royal Statistical Society: Series B (Statistical Methodology)*, vol. 61, no. 3, pp. 579–602, 1999.